VARIATION IN BANDWIDTHS AMONG SOLUTIONS TO SHAPED BEAM SYNTHESIS PROBLEMS CONCERNING LINEAR ARRAYS OF PARALLEL DIPOLES

J. C. Brégains (Student Member, IEEE), and F. Ares (Senior Member, IEEE)

Grupo de Sistemas Radiantes, Departamento de Física Aplicada,

Facultad de Física, Universidad de Santiago de Compostela.

15782 - Santiago de Compostela – SPAIN

faares@usc.es

ABSTRACT

The problem of synthesizing a linear array generating a shaped beam pattern with M filled nulls has 2^M alternative solutions. In this study we examined their bandwidths as regards compliance with pattern quality or input impedance requirements in the presence and absence of a backing ground plane. Placing a ground plane behind the antenna almost doubles side lobe level bandwidth.

1. INTRODUCTION

As is well known, the filled nulls of a shaped beam pattern generated by a linear array of N radiating elements spaced a distance d apart correspond to those roots of the equation

$$\sum_{n=1}^{N} I_n w^{n-1} = 0 \qquad (1)$$

that lie off the Schelkunoff unit circle, where I_n is the excitation of the n-th element and $w=\exp[j(2\pi d/\lambda)\cos\theta]$, with θ measured from endfire. It has often been pointed out [1-2] that any such off-circle root, $\exp(a_n + jb_n)$ say, can be replaced by $\exp(-a_n + jb_n)$ without altering the radiation power pattern. As a result, there are in general 2^M solutions for a pattern with M filled nulls, although the number of independent solutions will be smaller if symmetry constraints are introduced [2]. This multiplicity of solutions has in the past been taken advantage of by choosing from among their number the solution consisting of what appeared to be the excitation distribution least likely to be affected by problems due to mutual coupling among the elements, which in the case of dipole arrays has usually been identified as the one with the smallest value of $|I|_{\max}/|I|_{\min}$ or $(|I_n|/|I_{n\pm1}|)_{\max}$, where $|I|_{\max}$ and $|I|_{\min}$ are respectively the largest and smallest of the $|I_n|$.

In this work we investigated whether there can be solutions with significant advantages as regards bandwidth with respect to pattern quality or embedded impedance; compared the bandwidths of the 2^M solutions described above with those of a system consisting of a symmetric pure real excitation distribution generating a flat-topped beam of approximately equal width as in the above cases (for this it is necessary to introduce extra array elements [2]); and investigated the influence of a nearby ground plane on these findings. In all these calculations we considered an array of parallel dipoles spaced $\lambda/2$ apart.

2. METHOD

2.1 GENERAL SOLUTIONS IN THE ABSENCE OF A GROUND PLANE

We considered an array of 20 parallel dipoles of length $\lambda_D/2$ and radius 0.004763 λ_D, all parallel to the x axis and spaced λ_D /2 apart along the z axis, where λ_D is the design frequency. For this array we used the Orchard-Elliott method [1] to find a solution to the problem of synthesizing a symmetric flat-topped shaped beam pattern with M = 6 filled nulls, a beamwidth of about 52° between nulls, ± 0.5 dB of ripple, and a maximum side lobe level of -20 dB (Fig.1, continuous curve). This method directly affords the roots $\exp(a_n + jb_n)$ of eq.1, and we then found the other 63 excitation distributions giving the same radiation power pattern by generating all possible combinations of signs of the six nonzero a_n.

For each of the distributions $\{I_n\}$ so obtained, we next obtained the required input voltages V_n from the expression

$$V_n = \sum_{m=1}^{N} Z_{nm} I_m \qquad (2)$$

where the Z_{nm} are the self and mutual impedances of the elements, which were calculated as per Hansen [3]; and we then obtained the embedded impedances (or active impedances) $Z^e_n = V_n/I_n$. Finally, we investigated the tolerance of the solutions to deviations from the design frequency f_D as regards the embedded impedance characteristics $|Z_1^e|$, $|R_1^e|$, $|X_1^e|$, $|Z_{10}^e|$, $|R_{10}^e|$, $|X_{10}^e|$, $|Z^e|_{\max}$, $|R^e|_{\max}$ and $|X^e|_{\max}$ (where $Z^e_n = R^e_n + jX^e_n$) and the ripple, side lobe level and -3 dB beamwidth of the corresponding power patterns in the yz plane (φ = 90°). The impedances of the central element (10) and the edge element (1) were chosen for special attention because, like the present array, most shaped beam arrays have enough elements for the design to be based on these impedances. For each solution we fixed the V_n obtained above (arrays generating shaped beams are almost always designed on a constant voltage basis) and for each of a sequence of frequencies

differing by $\Delta f = f_D/300$ we calculated first the corresponding Z_{nm} (as per Hansen [3]) and then the corresponding I_m (by solving eqs.2) and the resulting power patterns (for which the array factor given by the I_n was multiplied by the element factor). By this means we determined $f_U = f_U^* - \Delta f$ and $f_L = f_L^* + \Delta f$ (where f_U^* and f_L^* are respectively the lowest frequency higher than f_D and the highest frequency lower than f_D at which the test characteristic differed by more than a specified amount δ from its value at f_D), and we calculated the bandwidth for the test characteristic in question as $(f_U - f_L)/f_D$, expressed as a percentage. For $|Z^e|_{max}$, $|R^e|_{max}$, $|X^e|_{max}$ and the corresponding properties of elements 1 and 10, the value of δ used was 15% of the values of these characteristics at f_D ; for the beamwidth at -3 dB, $\delta = \pm 2°$; for ripple, $\delta = \pm 0.5$ dB; and for the side lobe level, $\delta = \pm 3$ dB for levels higher than -20 dB and $\delta = \pm\infty$ otherwise.

2.2 PURE REAL SYMMETRIC SOLUTION IN THE ABSENCE OF A GROUND PLANE

To synthesize an array with a symmetric pure real excitation distribution generating a power pattern similar to that described above, we considered an array of 24 elements with eight off-circle roots $\exp(a_n + jb_n)$ of eq.1, each accompanied by both $\exp(a_n - jb_n)$ and $\exp(-a_n + jb_n)$ [2]; with this array size and these constraints the Orchard-Elliott method afforded a solution generating the pattern shown by the dotted curve in Fig.1 (increasing the number of double filled nulls broadened the beam excessively). For this solution we calculated the same bandwidths as described in the previous subsection, except that $|Z^e_{10}|$, $|R^e_{10}|$ and $|X^e_{10}|$ were replaced by $|Z^e_{12}|$, $|R^e_{12}|$ and $|X^e_{12}|$, elements 10 and 12 being central elements of the 20– and 24–element arrays, respectively.

2.3 SOLUTIONS IN THE PRESENCE OF A GROUND PLANE

All the calculations described above were repeated for the case of an array lying in the $y = \lambda_D/8$ plane with a ground plane occupying the $y = -\lambda_D/8$ plane. For this, the sets of excitations $\{I_n\}$ were taken to be the same as those found above, and input voltages and embedded impedances were calculated as described in [4] (pp.386 and 387). For bandwidth determinations, these calculated voltages were then fixed and the formulae of [4] were used to calculate excitation currents and embedded impedances. Fig.2 compares the patterns generated by 20-element $M = 6$ arrays with and without the ground plane.

3. RESULTS AND DISCUSSION

The main results are summarized in Table 1, in which letters in parentheses indicate whether the maximum- and minimum-bandwidth array current distributions are real (R) or complex (C), and also whether they are symmetric (S) or asymmetric (A).

In the absence of a ground plane, bandwidths for pattern ripple among the solutions for the 20-element array ranged from 13.33% (eight solutions) to 15.17% (two solutions, one of them the "all-outside" solution in which all the off-circle roots of eq.1 lie outside the unit circle). Side lobe level bandwidth ranged from 39.17% to 41.17%, and beamwidth bandwidth from 7.67% (two solutions, one of them one of the solutions with greatest ripple bandwidth) to 8.83%.

The relative variations in impedance bandwidths in the absence of a ground plane were more marked: $|Z^e|_{max}$ bandwidth ranged from 5.17% for the all-inside and all-outside solutions to 15.83%; $|R^e|_{max}$ bandwidth was in most cases between 11.17% and 23% (two solutions, one of them being one of the solutions with narrowest side lobe level bandwidth), although eight solutions had significantly narrower bandwidths ranging from 1.33% to 5.17% - this latter associated with the greatest beamwidth bandwidth; and $|X^e|_{max}$ bandwidth was in most cases between 1.33% (six solutions, one coinciding with the narrowest side lobe level bandwidth) and 6.83% (coinciding with the narrowest $|R^e|_{max}$ bandwidth), the exceptions in this case being the all-inside and all-outside solutions, which both had $|X^e|_{max}$ bandwidths of 24.67%. Almost all $|Z^e_1|$ bandwidths lay between 13.00% and 18.17% (the two exceptions were values of 8.83% - for the all-inside solution - and 9.83%); almost all $|R^e_1|$ bandwidths between 20.00% and 22.33% (the only exception being that of the all-inside solution, 18.83%); and all $|X^e_1|$ bandwidths between 1.00% and 2.17%. Almost all $|Z^e_{10}|$ bandwidths lay between 10.00% and 13.83% (the only exception being that of the all-inside solution, $|Z^e_{10}| = 5.50\%$); almost all $|R^e_{10}|$ bandwidths lay between 14.67% and 19.83% (seven were greater (20-24%) and two smaller (12.83% and 10%)**)**; and all $|X^e_{10}|$ bandwidths except two were either 1.00% or 0.67%, one of the exceptions being 0.83% and the other 3.00%.

Introducing a ground plane narrowed the ranges of $|R^e|_{max}$ and $|X^e|_{max}$ bandwidths among the 64 solutions: $|R^e|_{max}$ bandwidth now ranged from 7.67% to 19.00%**,** and $|X^e|_{max}$ bandwidth from 2.33% to 5.67% (in particular, the exceptionally high values of the all-inside and all-outside solutions were eliminated)**.** By contrast, the bandwidth range of $|Z^e|_{max}$, and those of $|Z^e_{10}|$, $|R^e_{10}|$, $|X^e_{10}|$, $|X^e_1|$, ripple and side lobe level, were all slightly widened. In the last four cases, however, the major effect of the ground plane was to raise the

whole range of bandwidths (from 13.33-15.17% to 14.67-19.33% for ripple, from 39.17-41.17% to 68.83-73.50% for side lobe level, from 1.00–2.17% to 2.33–4.00% for $|X^e_1|$ and from 0.67–3.00% to 1.00–4.50% for $|X^e_{10}|$ – no $|X^e_{10}|$ bandwidth was narrower with the ground plane than without); while for all solutions except five the major effect on $|Z^e_{10}|$ and $|R^e_{10}|$ bandwidths was to narrow them. The bandwidth ranges of $|Z^e_1|$ and $|R^e_1|$ were both narrowed and lowered, from 8.83–18.17% to 5.67–8.17% for $|Z^e_1|$, and from 18.33–22.33% to 8.67–11.67% for $|R^e_1|$. In many cases, but not all, the solutions with extreme bandwidth values in the presence of the ground plane also had extreme or near-extreme values in its absence.

Both of the solutions obtained for the 24-element array reflected the cost of imposing the condition that the excitations be both real and symmetric. In the absence of a ground plane**,** most of the bandwidth**s** were smaller than for the 20-element array or similar to the smaller values obtained for that array, with values of 8.67% for ripple, 30.33% for side lobe level, 4.33% for $|Z^e|_{\max}$, 3.33% for $|R^e|_{\max}$, 7.50% for $|Z_1{}^e|$, 16.50% for $|R^e_1|$ and 0.67% for $|X^e_{10}|$ (only $|X^e|_{\max}$ bandwidth, 13%, and $|X^e_1|$ bandwidth, 2.50%, were wider than for most 20-element solutions). In the presence of a ground plane, qualitatively the same differences with respect to the 20-element solutions were generally observed, the most significant deviation from this pattern being that side lobe level bandwidth, 73.67%, was now wider than for any 20-element solution.

4. CONCLUSIONS

The multiplicity of solutions generated by null filling does allow some choice as to the bandwidth of certain parameters of interest (notably $|X^e|_{\max}$ and $|Z^e|_{\max}$). Placing a ground plane behind the antenna almost doubles side lobe level bandwidth (to about 70%). Real symmetric solutions obtained by adding elements to the array generally have poorer bandwidth than solutions that are not both real and symmetric.

ACKNOWLEDGEMENTS

We thank Dr. R.C. Hansen for having suggested this research topic and for discussing its results at various stages. This work was supported by the Spanish Ministry of Science and Technology under project TIC 2002-04084-C03-02.

REFERENCES

[1] H. J. Orchard, R. S. Elliott, and G. J. Stern, “Optimising the synthesis of shaped beam antenna patterns”, *IEE Proceedings,* vol. 132, No. 1, pp. 63-69, Feb. 1985.

[2] Y. U. Kim, R. S. Elliott, “Shaped-Pattern Synthesis Using Pure Real Distributions”, *IEEE Trans. on Antennas and Propagat.*, Vol. 36, No. 11, pp. 1645-1649, Nov. 1988.

[3] R. C. Hansen, “Formulation of Echelon Dipole Mutual Impedance for Computer”, *IEEE Trans. on Antennas and Propagat.*, Vol. 20, No. 6, pp. 780-781, Nov. 1972.

[4] R. S. Elliott: “Antenna Theory and Design”, *IEEE-Press, Wiley-Interscience*, Revised Edition, 2003.

LEGENDS FOR THE FIGURES AND TABLES

Fig. 1. Continuous curve: a symmetric flat-topped shaped beam pattern with M = 6 filled nulls, a beamwidth of about 52° between nulls, ± 0.5 dB of ripple, and a maximum side lobe level of -20 dB generated by a 20-element $\lambda/2$-spaced linear array. Dotted curve: the similar pattern, with M = 8 filled nulls, generated by a 24-element $\lambda/2$-spaced linear array with a symmetric real excitation distribution.

Fig. 2. Continuous curve: the pattern shown as a continuous curve in Fig.1. Dotted curve: the pattern obtained when a ground plane is placed behind the antenna at a distance of $\lambda/4$ while antenna inputs are modified to maintain the same current distributions as before.

Table 1. Maximum and minimum bandwidths of every parameter considered.

Number of elements	Parameter	Without ground plane		With ground plane	
		Max	Min	Max	Min
20	**BW Ripple %**	15.17 (CS)	13.33 (CA)	19.33 (RA)	14.67 (CA)
	BW SLL[a] %	41.17 (CA)	39.17 (CS)	73.50 (CS)	68.86 (RA)
	BW -3dB %	8.83 (CA)	7.67 (CS)	8.50 (CA)	7.83 (CS)
	BW $\|Z^e\|_{max}$ %	15.83 (CA)	5.17 (RA)	15.67 (CS)	2.00 (RA)
	BW $\|R^e\|_{max}$ %	23.00 (RA)	1.33 (RA)	19.00 (CA)	7.67 (RA)
	BW $\|X^e\|_{max}$ %	24.67 (RA)	1.33 (CS)	5.67 (CA)	2.33 (RA)
	BW $\|Z^e_1\|$ %	18.17 (CA)	8.83 (RA)	8.17 (RA)	5.67 (RA)
	BW $\|R^e_1\|$ %	22.33 (CA)	18.83 (RA)	11.67 (CA)	8.67 (RA)
	BW $\|X^e_1\|$ %	2.17 (RA)	1.00 (CA)	4.00 (RA)	2.33 (CA)
	BW $\|Z^e_{10}\|$ %	13.83 (RA)	5.50 (RA)	18.50 (CA)	4.33 (RA)
	BW $\|R^e_{10}\|$ %	24.00 (CS)	10.00 (RA)	20.50 (CA)	4.50 (RA)
	BW $\|X^e_{10}\|$ %	3.00 (RA)	0.67 (CA)	4.50 (RA)	1.00 (CA)
24 (RS)	**BW Ripple %**	8.67		10.17	
	BW SLL[a] %	30.33		73.67	
	BW -3dB %	8.17		8.00	
	BW $\|Z^e\|_{max}$ %	4.33		3.17	
	BW $\|R^e\|_{max}$ %	3.33		9.00	
	BW $\|X^e\|_{max}$ %	13.00		3.50	
	BW $\|Z^e_1\|$ %	7.50		5.33	
	BW $\|R^e_1\|$ %	16.50		7.83	
	BW $\|X^e_1\|$ %	2.50		4.00	
	BW $\|Z^e_{10}\|$ %	11.50		9.17	
	BW $\|R^e_{10}\|$ %	16.50		12.67	
	BW $\|X^e_{10}\|$ %	0.67		2.00	

[a] SLL = side lobe level.

Table 1.

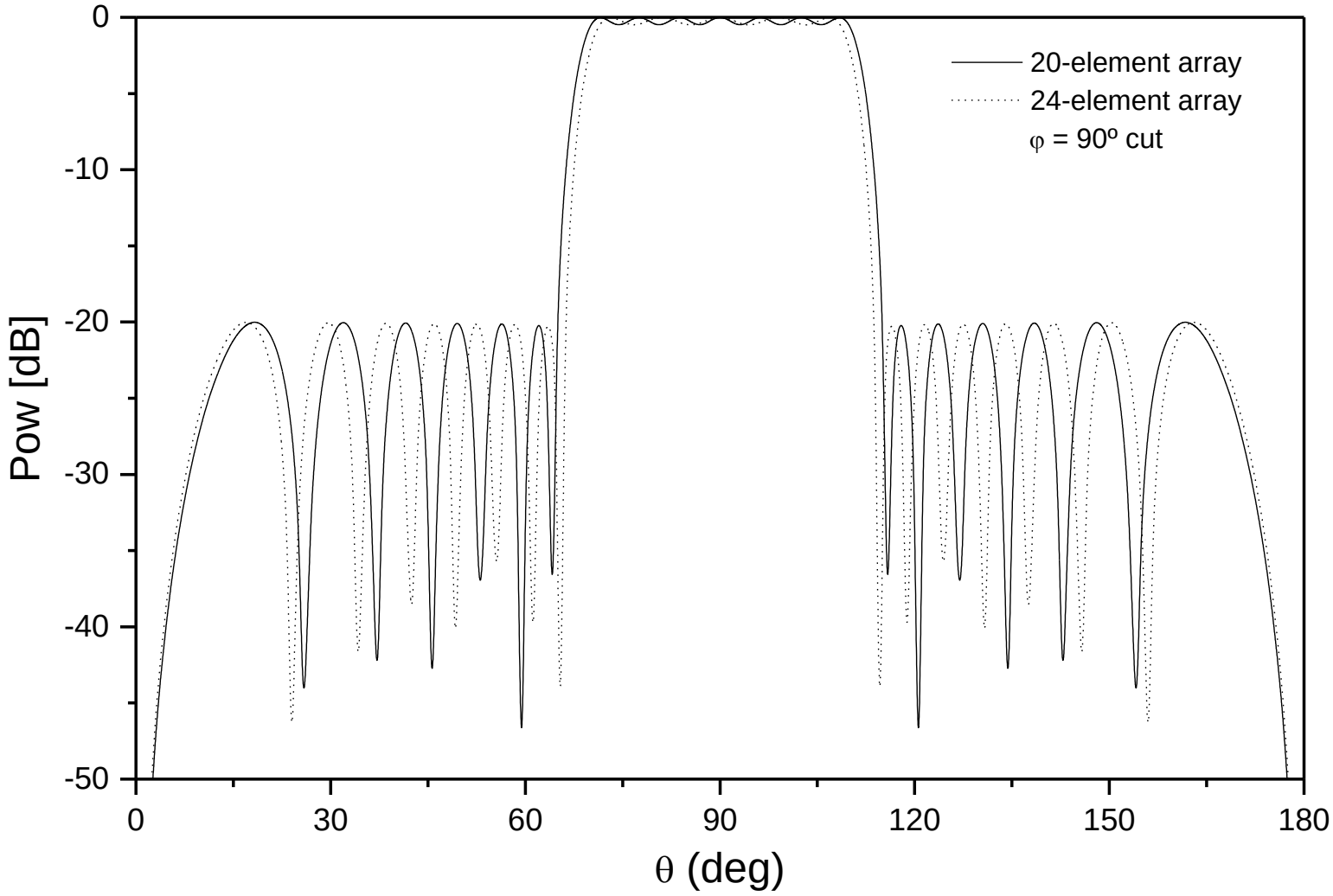
0
-10
-20
-30
-40
-50
Pow [dB]
0
30
60
90
120
150
180
θ (deg)
20-element array
24-element array
φ = 90º cut

Fig. 1

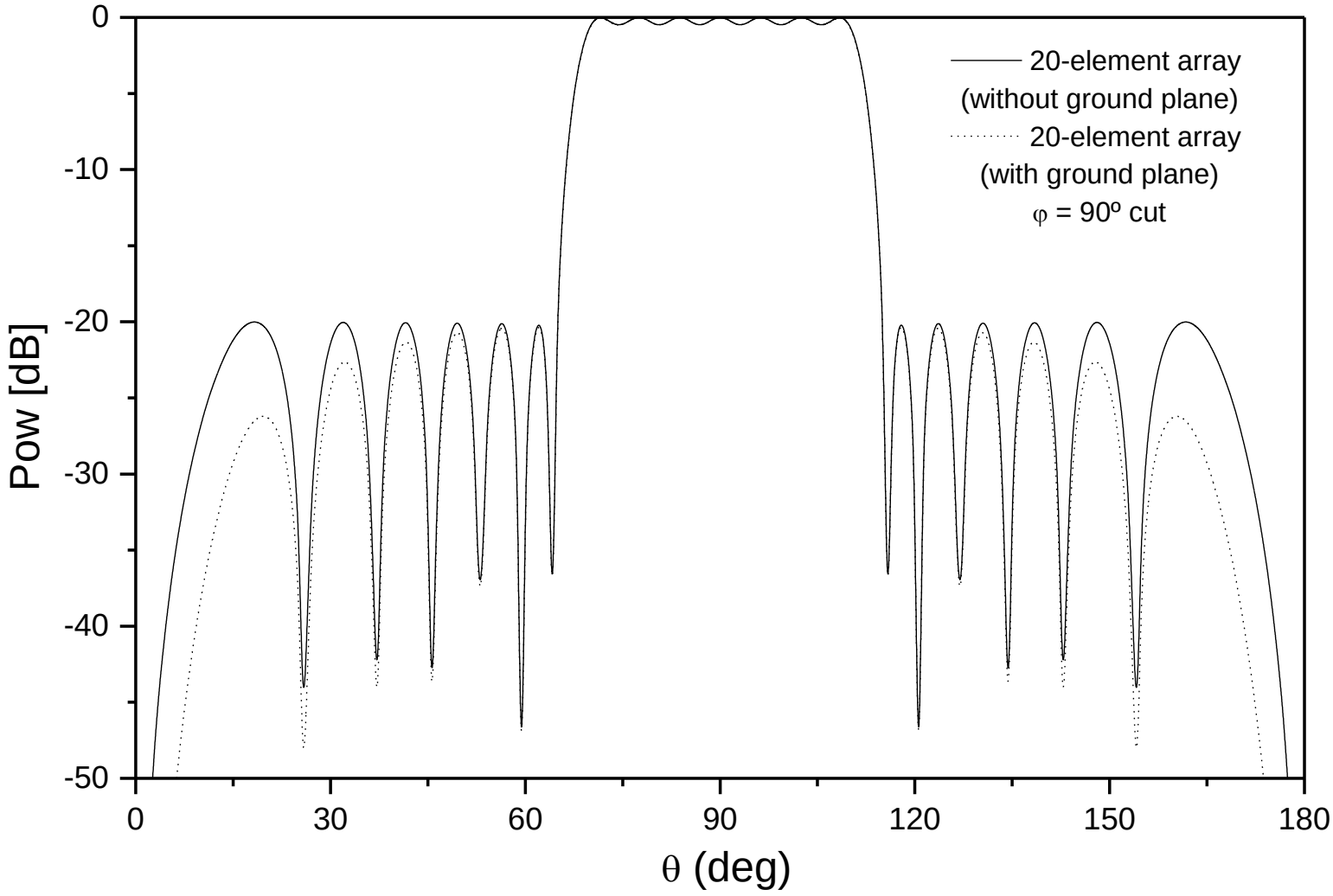
0
-10
-20
-30
-40
-50
Pow [dB]
0
30
60
90
120
150
180
θ (deg)
20-element array
(without ground plane)
20-element array
(with ground plane)
φ = 90º cut

Fig. 2